

Characterization of ternary $\text{Ti}_x\text{V}_{1-x}\text{N}_y$ nitride prepared by mechanosynthesis.

M.A.Roldán, M.D.Alcalá, C.Real*

Instituto de Ciencia de Materiales de Sevilla. Centro mixto US-CSIC. Av.Américo Vespucio nº49.
41092-Sevilla (Spain)

Keywords: mechanosynthesis, XAS, EELS, microhardness, ternary nitride

Abstract

In the present manuscript the authors have systematically investigated the composition and microstructure of a series of ternary nitrides ($\text{Ti}_x\text{V}_{1-x}\text{N}_y$) ($0.0 \leq x \leq 1.0$) prepared by mechanosynthesis, using XRD, SEM, EELS, XAS and TGA. The ternary titanium-vanadium nitride ($\text{Ti}_x\text{V}_{1-x}\text{N}_y$) has been obtained in all range of compositions by the mechanical treatment of the two metals under nitrogen pressure in a planetary mill with a maximum milling time of 3 h and without any post-heating treatment. The materials' microhardnesses were measured after sinterisation and compared to those reported in literature for these types of materials. When compared with the previously reported data for bulk samples, these values are similar or higher for compositions within the range $x = 0.5$ to $x = 0.77$ ($\text{Ti}_x\text{V}_{1-x}\text{N}$).

1. Introduction

Traditional applications of metal nitrides include cutting tools, structural materials [1,2] magnetic and electric components [3], superconducting devices [4,5] and industrial catalysts [6,7]. Ternary transition metal nitrides exhibit similar, and sometimes improved, properties to those of binary nitrides when used as electrode materials for supercapacitors and catalysts. Structural and compositional control of these materials may exert a crucial influence on their overall performance, and the formation of ternary metal nitrides may widely expand the properties of this class of materials. Despite many years of intensive effort by several research groups, the number of known ternary nitrides is trivial if compared with the known ternary oxides or sulphides. This difference is clearly due to the difficult synthesis of ternary nitrides and also to their instability with respect to that of oxides. However, after several decades of dedicated research, advances in inorganic nitride chemistry have accelerated

* Author to whom correspondence should be addressed. e-mail: creal@icmse.csic.es

1
2
3
4
5
6
7
8
9
10
11
12
13
14
15
16
17
18
19
20
21
22
23
24
25
26
27
28
29
30
31
32
33
34
35
36
37
38
39
40
41
42
43
44
45
46
47
48
49
50
51
52
53
54
55
56
57
58
59
60
61
62
63
64
65

dramatically over the past 5–10 years, and novel synthetic strategies have been developed. The traditional synthetic methods for generating these types of compounds include the amonolysis of ternary oxides [8,9] and metal alloys [10-12]; solid state reactions using chlorides, nitrates, and pre-structured oxides [13-19]; and deposition methods [20-25]. Information in the literature concerning titanium-vanadium nitride has shown the superior performance of such coated ternary compounds to those of both pure TiN and VN, with respect to their hardnesses and tribological environments [26-38]. A small addition of vanadium to titanium nitride improved the supercapacitor properties of TiN [39]. Traditionally, titanium and vanadium nitrides have been synthesised as thin films using different deposition methods, such as cathodic arc deposition [31], cathodic magnetron sputtering [32], reactive magnetron sputtering [33-35], or chemical vapour deposition, [36-38,40,41] or by the direct nitridation of metal alloys [42-45]. To our knowledge, only two works have reported the preparation of $Ti_xV_{1-x}N_y$ in bulk. Fischer et al. [46] obtained this compound by infiltrating a mixture containing the two precursor metals into mesoporous carbon nitride, heating and then decomposing the carbon nitride. In that study, mesoporous graphitic carbon nitride was used as both a nanoreactor and a reactant for the synthesis of ternary metal nitride nanoparticles. Moreover, we have previously demonstrated that this material could be obtained from the carbothermal reduction of oxide mixtures under a nitrogen atmosphere [47].

In the present study, we synthesised pure titanium-vanadium nitride by mechanically treating the two metals under nitrogen pressure, in a planetary mill and with a milling time of 3 h; no post-heating treatment was applied. The final products obtained from this method were characterised and compared with the final products obtained using a thermal procedure.

2. Experimental

2.1. Materials:

Vanadium (V) [262935, 99.5 %, < 325 mesh, Aldrich], Titanium (Ti) [93-2267, 99 %, < 325 mesh, Strem Chemicals] and nitrogen gas (N_2) [pure, $H_2O \leq 3$ ppm, $O_2 \leq 2$ ppm, $y C_nH_m \leq 0.5$ ppm, Air Liquide] were used as precursors.

2.2. Methods:

V and Ti powders were milled under the pressure of high purity N_2 at 11 bars using a modified planetary ball mill (Fritsch, model Pulverisette 7). A steel vial of 45 cm^3 was used with 6 steel balls and 5 g of metal mixture. The diameter and the weight of the

1 balls were 15 mm and 13.85 g, respectively, and the powder-to-ball mass ratio was
2 1:16. The vial was purged with N₂ several times, and the desired N₂ pressure was then
3 adjusted prior to milling. The vial and the gas cylinder were connected through a rotary
4 valve and a flexible polyamide tube, which allowed working pressures up to 27 bars.
5 The rotary valve can operate up to 25000 rpm under pressures ranging from vacuum to
6 70 bars. As such, the vial is permanently connected to the gas cylinder that supplies gas
7 at its desired pressure throughout the entire process. A rotation rate of 700 rpm was
8 always employed for the supporting disc and the superimposed vial in the opposite
9 direction.
10

11
12
13
14
15
16
17
18
19
20
21
22
23
24
25
26
27
28
29
30
31
32
33
34
35
36
37
38
39
40
41
42
43
44
45
46
47
48
49
50
51
52
53
54
55
56
57
58
59
60
61
62
63
64
65

Characterization of the final products (ternary nitrides) was performed using the following techniques:

2.2.1. X-ray powder diffraction (XRD). Patterns were collected with a Siemens D501 instrument equipped with a scintillation counter using Cu K_α radiation and a primary graphite monochromator. The goniometer scanning rate was of 0.4 °min⁻¹. The average diameter of the coherently diffraction domain was calculated with the Scherrer method [48] using the (200) diffraction peak of Ti_xV_{1-x}N_y. The lattice parameter refinement corresponding to the final product was also calculated from the entire set of XRD peaks using the Lapods computer program [49] and assuming a cubic symmetry for Ti_xV_{1-x}N_y.

2.2.2. The iron content contamination of the milling samples was analysed by permanganimetry.

2.2.3. The composition analysis was performed with a high-resolution transmission electron microscope (HRTEM, Philips CM200, Eindhoven) with a super twin objective lens and working at 200 kV with a LaB₆ filament. The instrument is equipped with a parallel electron energy loss spectrometer (EELS, Model 766-2K, Gatan, München, Germany). For its observation, the sample was embedded in a resin, then a film of 100 nm was cut and the sample was supported on a holey carbon grid. The N, Ti and V core-loss edges were recorded in the diffraction mode with a camera length of 470 mm using a 2-mm spectrometer. The entrance aperture yielded an energy resolution at a zero-loss peak of 1.4 eV. The spectra were recorded for dark current and channel-to-channel gain variation. After subtracting the background using a standard power-law function, the spectra were deconvoluted for plural scattering applying the Fourier-ratio

method and normalised to the jump. All of these treatments were performed within the EL/P program (Gatan).

2.2.4. The X-ray absorption spectra (XAS) at Ti-K ($E = 4965$ eV) and V-K ($E = 5465$ eV) edges for the sample $\text{Ti}_{0.5}\text{V}_{0.5}\text{N}_{0.94}$ were recorded at the synchrotron radiation source ESRF in Grenoble, France, at station BM29. The ring energy was 6 GeV, and the maximum stored current was 200 mA. A double crystal Si (311) monochromator was used. Higher harmonic rejection was performed by detuning both crystals by 50 % of the intensity of the first harmonic. Measurements were conducted at room temperature in the transmission detection mode using detectors with 45-cm ionisation chambers that were filled with the appropriate gas mixtures. The amount of sample used was calculated to attain the optimal absorption of $\mu x = 2.5$. Because the required amount of sample was rather small (a few milligrams), it was mixed with BN to reach the minimum size to construct a self-supporting pellet.

2.2.5. Microstructural observations were conducted using scanning electron microscopy (SEM, model JSM 5400 Jeol). The images were recorded at 30 kV. The sample powders were dispersed in ethanol and supported on a metallic grid.

2.2.6. Vickers microhardness measurements (FM-700, Future-Tech, Hardness tester) were conducted on the pellet cross-sections under a load of 1 kgf for 15 s. The average microhardness was calculated from 20 indents per specimen.

3. Results and discussion

A range of ternary titanium vanadium nitride ($\text{Ti}_x\text{V}_{1-x}\text{N}_y$) composites have been prepared by milling a mixture of these metals for different time periods under nitrogen pressure (11 bars). Figure 1 shows the XRD pattern of the $\text{Ti}_{0.50}\text{V}_{0.50}\text{N}_{0.94}$ sample at different grinding times and the pattern corresponding to the starting metals as well. The XRD patterns indicated that titanium vanadium nitride was formed from the mixture of the two metals by milling under nitrogen. XRD diagrams that represent 0 to 165 min of milling time showed Ti and V peak broadening that increased with milling time due to the refinement of the crystallite size and the formation of defects and microstrains. Moreover, the grinding between 120 and 165 min showed emergent diffraction peaks at $2\Theta = 37$ and 43 that correspond to a ternary nitride (JCPDF-89-5212). When grinding time was increased in 15 min, thus reaching 180 min, the XRD patterns evidenced only

1 ternary nitride peaks. This result confirms that the reaction proceeded through a
2 combustion-like process (MSR). To verify this particular, the nitrogen pressure was
3 continuously monitored during the milling process by a SMC Solenoid Valve (model
4 EVT307-5DO-01FQ, SMC Co.) that was connected to a data acquisition system
5 ADAM-4000 series (Advantech Co. Ltd.). When the MSR occurred, the increasing
6 temperature induced by the exothermic reaction produced an instantaneous increase in
7 the total pressure. The ignition time of the sample (e.g., the milling time required to
8 produce the combustion process) is deduced from the time–pressure record, being about
9 172 min. Additional grinding causes an increase in the nitrogen content and diffraction
10 peaks broaden.
11
12
13
14
15
16
17

18 Figure 2 shows the XRD pattern of sample $Ti_{0.75}V_{0.25}N_{0.96}$. When a grinding time of
19 4 h is applied, the nitridation reaction is initiated. The reaction continues gradually but
20 doesn't get completed after 9 h of milling. This result confirms that the reaction occurs
21 through a diffusion process.
22
23
24

25 Table 1 lists the different ternary nitride compositions, process type, ignition time
26 and grinding time. It was possible to obtain a wide range of composites with different
27 mechanisms.
28
29
30

31 The actual compositions were obtained by EDX using the SEM. The iron content
32 contamination of the milling samples was analysed by permanganometry, reaching a
33 maximum value of 2.5 %. The iron was completely removed by rinsing the samples
34 with diluted hydrochloric acid. The nitriding percentage was calculated by
35 thermogravimetric analysis (TGA), an indirect method of analysis. The TGA diagrams
36 for the samples were recorded from room temperature to 1500 °C, at a heating rate of 5
37 K/min, using a nitrogen flow of 150 cm³/min and at a pressure of 1 bar. The nitriding
38 percentage was calculated from the mass gain, assuming a stoichiometric nitride as the
39 final product; all results are shown in Table 2.
40
41
42
43
44
45
46

47 The considerable broadening of the ternary nitride XRD peaks in all cases suggests
48 that this phase always exhibited a very refined microstructure. The crystallite size of the
49 final product was estimated using the Scherrer equation, and the values are included in
50 Table 3. The solid state reactions induced by ball milling occurred during the collisions
51 between balls and the powder. The reaction progressed through multiple events with
52 very short reaction times. Under these conditions, crystal growth of the new phase was
53 hindered, generally leading to products with a nanometre microstructure. The dimension
54 of the $Ti_xV_{1-x}N_y$ cubic unit cell was determined from the entire set of XRD peaks
55
56
57
58
59
60
61
62
63
64
65

1 recorded for 2θ values ranging from 10° to 90° . Least squares fitting of the XRD peaks
2 was conducted with Lapods program, and the values are shown in Table 3. The lowest
3 value obtained for the lattice parameters as compared with de Vegard's results, suggests
4 that a nonstoichiometric compound was obtained, and this value is in good agreement
5 with the nitrogen percentage shown in Table 2. Studies for several transition metals
6 with composition MN_x [50-52] have reported that the a parameter is very sensitive to
7 the nitridation level.
8

9
10
11
12 The nitrogen content in the ternary nitride composites was also calculated using
13 EELS analysis by recording core-level absorption edges at a microscopic level. Figure 3
14 shows the N-K, Ti-L₂₋₃ and V-L₂₋₃ edges for the different samples prepared in this
15 present work. The N-K edge peak is exhibited in all samples with the same shape,
16 indicating that the materials share the same homogeneous structure and zones with
17 similar elemental atomic ratios. The composition of the materials was determined by
18 integrating the number of counts under the peaks and employing the relevant cross-
19 sections that were provided by Gatan EL/P software. The representative results from the
20 quantitative analysis performed from Figure 3 are shown in Table 4. The EDX and TGA
21 values are also listed in Table 4. These results are in good agreement, and the small
22 discrepancies between the EELS and TGA values might be explained by a percentage of
23 the sample undergoing amorphisation; this is possible because the mechanosynthesis
24 method employed induces a high degree of amorphisation. Thus, $Ti_{0.5}V_{0.5}N_{0.94}$ was also
25 characterised by XAS analysis; this technique can analyse both crystalline and
26 amorphous samples. The normalised XANES spectra for the Ti-K and V-K absorption
27 edges appeared at 4966 and 5465 eV, respectively (Figure 4). The Ti-K and V-K edges
28 are sensitive to the coordination environment and the oxidation states of Ti and V
29 compounds. Therefore, the overall shape of this material was used as a fingerprint and
30 compared with the shapes of other crystalline compounds with known structure [53].
31 The XANES data are similar to the spectrum obtained for TiN and VN compounds. The
32 EXAFS oscillation intensity of the spectra is rather low, indicating that these samples
33 should exhibit a high degree of amorphisation. The spectra for the starting models
34 corresponded to the crystalline structures of the species Ti-bcc, V-bcc, TiN-fcc and VN-
35 fcc. A single free parameter a , which is the lattice parameter, was used to allow the
36 coherent variation of the coordination distances for all coordination shells. The
37 respective coordination numbers were fixed to those of perfect crystal structures. The
38 Debye-Waller factors (σ^2) were allowed to vary independently for each coordination
39
40
41
42
43
44
45
46
47
48
49
50
51
52
53
54
55
56
57
58
59
60
61
62
63
64
65

1 shell. Due to the highly distorted nature of these milled samples, the static disorder
2 caused by the deformation from the ideal structure induced a coordination distance
3 spread around the average values. This large disorder is due to the large number of
4 defects, and a detailed explanation of the adjustment of the disorder is reported in a
5 previous work [54]. This variable (D) ranges from 0, for a sample with atoms lacking
6 any order even in the first coordination shell, to 1, if the sample is a perfect crystal. A
7 summary of the results is given in Tables 5 and 6. These results are in good agreement
8 with the results from X-ray analysis shown in Table 3.

9
10
11
12
13
14 To complete the characterisation, a morphology study of the different samples
15 was performed using SEM. Figure 5 displays SEM images illustrating the morphologies
16 of three prepared samples. The microstructures of all samples were similar, being
17 characterised by agglomerated grains with sizes ranging from 0.2 to 1 μm , formed by
18 highly dense, spherical, nanometre sized particles.

19
20
21
22
23
24 Finally, the samples were sintered to measure their microhardness. First, green
25 bodies were obtained as pellets that contained 400 mg of sample by isostatic pressing.
26 The samples were then sintered at 1750 $^{\circ}\text{C}$ for 1 h under a helium atmosphere. The
27 morphology studies for the different samples are shown in Figure 5. A large
28 densification, approaching full density, was observed (Table 7). The microhardness
29 values of the current samples and those of samples previously reported using a thermal
30 method are also shown in Table 7 [47]. These data are in good agreement with the
31 microhardness-composition relationship, as demonstrated in the literature [28-32,35-
32 36,55-56] for these materials. The above cited authors have shown that the
33 compositions between $x = 0.5$ and 0.77 ($\text{Ti}_x\text{V}_{1-x}\text{N}$) correspond to the materials with the
34 highest microhardness and that the best microhardness results correlate to sample
35 compositions with high stoichiometry. Additionally, the microhardness values for the
36 ternary nitride composites were lower than those obtained by these authors (2000-4000
37 Hv). However, all of these results correspond to films, and it is known that dense films
38 with a high defect concentration can produce microhardness values far above those
39 corresponding to bulk samples [55]. When these values are compared with some others
40 previously studied for bulk samples [47], it can be seen that they are similar or higher
41 for the compositions between $x = 0.5$ and 0.77 ($\text{Ti}_x\text{V}_{1-x}\text{N}$).

4. Conclusions

1 Bulk samples of ternary nitrides ranging in different compositions were rapidly obtained
2 by mechanical treatment at room temperature. The materials richest in titanium and
3 vanadium were produced through a combustion process in 3 h and a diffusion process in
4 9 h, respectively. Reactive milling is a good method to obtain these types of compounds
5 because it is inexpensive if compared with deposition and thermal techniques. The
6 employed characterisation methods indicate that the materials exhibited nanometre
7 particle sizes, high sinterabilities and high microhardnesses.
8
9
10
11
12
13
14

15 References

- 16
17 [1] S.T.Oyama, The chemistry of transition metal carbides and nitrides, edited by Blackie
18 Academic & Professional. Glasgow, Scotland, (1996) pp 1-52.
19 [2] L.E.Toth, Transition metal carbides and nitrides, edited by Academic Press, New York,
20 (1971).
21 [3] N.Pessall, R.E.Gold, H.A.Johansen, A study of superconductivity in interstitial
22 compounds, *J.Phys.Chem.Solids*, 29 (1968) 19-27.
23 [4] R.M.Powell, W.Skocpol, M.Tinkham, Preparation and superconducting properties of
24 ultrafine powders and sintered compacts of nbc and nbn, *J.Appl.Phys.*, 48[2] (1977) 788-
25 799.
26 [5] T.Yamada, M.Shimada, M.Koizumi, Fabrication and characterization of titanium nitride
27 by high-pressure hot-pressing, *Ceram.Bull.*, 59[6] (1980) 611-616.
28 [6] S.T.Oyama, Preparation and catalytic properties of transition-metal carbides and nitrides,
29 *Catal.Today*, 15[2] (1992) 179-200.
30 [7] H.Kwon, S.Choi, L.T.Thompson, Vanadium nitride catalysis: synthesis and evaluation for
31 n-butane dehydrogenation, *J.Catal.*, 184 (1999) 236-246.
32 [8] P.S. Herle, N.Y.Vassanthacharya, M.S.Hegde, M.S.Gopalakrishnan, Synthesis of new
33 transition-metal nitrides, *mwn(2)* (m=mn, co, ni), *J.Alloys Comp.* 217[1] (1995) 22-24.
34 [9] A.Gomathi, Ternary metal nitrides by the urea route, *Mater.res.Bull.*, 42[5] (2007) 870-
35 874.
36 [10] P.Krawiec, R.N.Panda, E.Kockrick, D.Geiger, S.Kaskel, High surface area V-Mo-N
37 materials synthesized from amine intercalated foams, *J.Solid State Chem.*, 181 (2008)
38 935-942.
39 [11] S.Korlann, B.Diaz, M.E.Bussell, Synthesis of bulk and alumina-supported bimetallic
40 carbide and nitride catalysts, *Chem.Mater.*, 14[10] (2002) 4049-4058.
41 [12] C.J.H.Jacobsen, Novel class of ammonia synthesis catalysts, *Chem.commun.*, 12 (2000)
42 1057-1058.
43 [13] K.S.Weil, P.N.Kunta, J.Grins, Revisiting a rare intermetallic ternary nitride, Ni₂Mo₃N:
44 Crystal structure and property measurements, *J.Solid State Chem.*, 146[1] (1999) 22-35.
45 [14] A.El-Himri, P.Nuñez, F.Sapiña, R.Ibañez, A.Beltran, J.M.Martinez-Agudo, Synthesis of
46 new molybdenum-tungsten, vanadium-tungsten and vanadium-molibdenum-tungsten
47 oxynitrides from freeze-dried precursors, *J.Solis.State.Chem.*, 177 (2004) 2413-1431.
48 [15] Z.A.Gal, L.Cario, F.J.DiSalvo, "Synthesis, structure and magnetic properties of the ternary
49 nitride La₃V₂N₆", *Solid State Sci.*, 5[7] (2003) 1033-1036.
50 [16] R.Niewa, D.Zherebtsov, Z.Hu, Polymorphism of heptalithium
51 nitridovanadate(V)Li₇[VN₄], *Inorg.Chem.*, 42[8] (2003) 2538-2544.
52 [17] M.T.Barker, M.G.Francesconi, P.M.O'Meara, C.F.Baker, New synthetic routes to
53 transition metal ternary nitrides and sulfides, *J.alloys comp.*, 317-318 (2001) 186-189.
54 [18] S,Alconchel, F.Sapiña, D.Beltran, A.Beltran, A new approach to the synthesis of
55 molybdenum bimetallic nitrides and oxynitrides, *J.Mater.Chem.*, 9 (1999) 749-755.
56
57
58
59
60
61
62
63
64
65

- 1 [19] A.El-Himri, P.Nuñez, F.Sapiña, A.Beltran, Freeze-dried precursor-based synthesis of new
2 polymetallic oxynitrides, $V_{1-u-z}Cr_uMo_z(O_xN_y)$, $V_{1-u-z}Cr_uW_z(O_xN_y)$, $Cr_{1-u-z}Mo_uW_z(O_xN_y)$
3 ($u,z=0.2,0.33,0.4,0.6$, $u+z<1$), and $V_zCr_zMo_z(O_xN^y)$ ($z=0.25$), *J.Alloys comp.*, 398 (2005)
4 289-295.
- 5 [20] H.Hasegawa, T.Suzuki, Effects of second metal contents on microstructure and micro-
6 hardness of ternary nitride films synthesized by cathodic arc method, *Surf.Coating*
7 *Technol.*, 188 (2004) 234-240.
- 8 [21] J.V.Ramana, S.Kumar, C.David, V.S.Raju, Structure, composition and microhardness of
9 (Ti,Zr)N and (Ti,Al)N coating prepared by DC magnetron sputtering, *Mater.Lett.*, 58
10 (2004) 2553-2558.
- 11 [22] M.B.Takeyama, T.Itoi, E.Aoyagi, A.Noya, Diffusion barrier properties of nano-crystalline
12 TiZrN films in Cu/Si contact systems, *Appl.Sur.Sci.*, 216 (2003) 181-186.
- 13 [23] S.M.Aouadi, J.A.Chalek, N.Namavar, N.Finnegan, S.L.Rohde, Characterization of Ti-
14 based nanocrystalline ternary nitride films, *J.Vac.Sci. Technol.B*, 20[5] (2002) 1967-1973.
- 15 [24] R.L.Boxman, V.N.Zhitomirsky, I.Grimberg, L.Rapoport, S.Goldsmith, B.Z.Weiss,
16 Structure and hardness of vacuum arc deposited multi-component nitride coating of Ti, Zr
17 and Nb, *Surf.Coating Technol.*, 125 (2000) 257-262.
- 18 [25] P.Hones, R.Sanjines, F.Levy, Electronic structure and mechanical properties of resistant
19 coatings: The chromium molybdenum nitride system, *J.Vac.Sci.Technol.A*, 17[3] (1999)
20 1024-1030.
- 21 [26] J.H.Ouyang, S.Sasaki, The friction and wear characteristics of cathodic arc ion-plated
22 (V,Ti)N coatings in sliding against alumina ball, *Wear*, 257[7-8] (2004) 708-720.
- 23 [27] J.H.Ouyang, S.Sasaki, Tribo-oxidation of cathodic arc ion-plated (V,Ti)N coatings sliding
24 against a steel ball under both unlubricated and boundary-lubricated conditions,
25 *Surf.Coatings Technol.*, 187[2-3] (2004) 343-357.
- 26 [28] N.Ichimiya, Y.Onishi, Y.Tanaka, Properties and cutting performances of (Ti,V)N coatings
27 prepared by cathodic arc ion plating, *Surf.Coatings Technol.*, 200 (2005) 1377-1382.
- 28 [29] K.E.Davies, B.K.Gan, D.R.McKenzie, M.M.M.Bilek, M.B.Taylor, D.G.McCulloch,
29 B.A.Latella, Correlation between stress and hardness in pulsed cathodic arc deposited
30 titanium/vanadium nitride alloys, *J.Phys.Condes.Mater*, 16 (2004) 7947-7954.
- 31 [30] H.Hasegawa, A.Kimura, T.Suzuki, Microhardness and structural analysis of (Ti,Al)N,
32 (Ti,Cr)N, (Ti,Zr)N and (Ti,V)N films, *J.Vac.Sci.Technol.A*, 18[3] (2000) 1038-1040.
- 33 [31] O.Knotek, W.Burgmer, C.Stoessel, Arc-evaporated Ti-V-N thin films, *Surf.Coatings*
34 *Technol.*, 54-55 (1992) 249-254.
- 35 [32] B.A.Latella, B.K.Gan, K.E.Davies, D.R.McKenzie, D.G.McCulloch, Titanium
36 nitride/vanadium nitride alloy coatings: mechanical properties and adhesion characteristics,
37 *Surf.Coatings Technol.*, 200 (2006) 3605-3611.
- 38 [33] Q.Luo, Z.Zhou, W.M.Rainforth, P.Eh.Hovsepian, TEM-EELS study of low-friction
39 superlattice TiAlN/VN coating: the wear mechanisms, *Tribology letters*, 24[2] (2006) 171-
40 178.
- 41 [34] U.Helmersson, S.Todoroya, S.A.Barnett, J.E.Sundgren, L.C.Market, J.E.Greene, Growth
42 of single-crystal TiN/VN strained-layer superlattices with extremely high mechanical
43 hardness, *J.Appl.Phys.*, 62[2] (1987) 481-484.
- 44 [35] O.Knotek, A.Barimani, B.Bosserhoff, F.Löffler, Structure and properties of magnetron-
45 sputtered Ti-V-N coatings, *Thin Solid Films*, 193-194 (1990) 557-564.
- 46 [36] R.Sanjines, C.Wierner, P.Hones, F.Levy, Chemical bonding and electronic structure in
47 binary VN_y and ternary $Ti_{1-x}V_xN_y$, *J.Appl.Phys.* 83[3] (1998) 1396-1402.
- 48 [37] I.L.Singer, S.Fayeulle, P.D.Ehni, Friction and wear behaviour of TiN in air; The chemistry
49 of transfer films and debris formation, *Wear*, 149[1-2] (1991) 375-394.
- 50 [38] K.N.Jallad, D.Ben-Amotz, Raman chemical imaging of tribological nitride coated (TiN,
51 TiAlN) surfaces, *Wear*, 252[11-12] (2002) 956-969.
- 52 [39] D.Choi, P.N.Kunta, Nanocrystalline TiN derived by a two-step halide approach for
53 electrochemical capacitors, *J.Electrochem.Soc.*, 153[12] (2006) A2298-A2303.
- 54 [40] M.Stoiber, E.Badisch, C.Lugmair, C.Mitterer, Low-friction TiN coatings deposited by
55 PACVD, *Surf.Coatings Technol.*, 163-164 (2003) 451-456.
- 56
57
58
59
60
61
62
63
64
65

- 1 [41] K.H.Habig, Chemical vapour deposition and physical vapour deposition coatings:
2 properties, tribological behaviour and applications, *J.Vac.Technol.A*, 4[6] (1986) 2832-
3 2843.
- 4 [42] S.Malinov, A.Zhecheva, W.Sha, Nitriding of titanium and aluminium allotys, *Metal*
5 *Sci.Heat Treatment*, 46[7-8] (2004) 286-293.
- 6 [43] J.A.Garcia, G.G.Fuentes, R.Martinez, R.J.Rodriguez, G.Abrasonis, J.P.Riviere, J.Rius,
7 Temperature-dependent tribological properties of low-energy N-implanted V5Ti alloys,
8 *Surf.Coatings Technol.*, 188-189 (2004) 459-465.
- 9 [44] J.A.Garcia, G.G.Fuentes, R.Martinez, A.Medrano, M.Rico, R.Rodriguez, M.Varela,
10 I.Colera, D.Caceres, I.Vergara, C.Ballesteros, E.Roman, J.L.de segovias, Surface
11 mechanical effects of nitrogen ion implantation on vanadium alloys, *Surf.Coatings*
12 *Technol.*, 158-159 (2002) 669-673.
- 13 [45] T.Yokoyama, K. Kobayashi, T. Ohta, A. Ugawa, Anharmonic interatomic potentials of
14 diatomic and linear triatomic molecules studied by extended x-ray-absorption fine structure,
15 *Phys.Rev.B*, 53[10] (1996) 6111-6112.
- 16 [46] A.Fischer, J.O.Müller, M.Antonietti, A.Thomas, Synthesis of Ternary Metal Nitride
17 Nanoparticles Using Mesoporous Carbon Nitride as Reactive Template, *ACS Nano*, 2(12) (
18 2008) 2489-2496.
- 19 [47] M.A. Roldán, M.D. Alcalá, A. Ortega, C. Real, Síntesis y caracterización del nitruro
20 ternario de titanio y vanadio ($Ti_xV_{1-x}N$), *Bol.Soc.Esp.Ceram.V.* 50[1] (2011) 31-40.
- 21 [48] L.E. Alexander, H.P. Klung, X-Ray Diffraction Procedures: for polycrystalline and
22 amorphous materials, edited by John Wiley & Sons, New York, (1974) pp. 618.
- 23 [49] C. Dong Y J. I. Langford, LAPODS: a computer program for refinement of lattice
24 parameters using optimal regression, *J. Appl. Cryst.* 33 (2000) 1177-1179.
- 25 [50] M.D. Aguas, A.M. Nartowski, I.P. Parkin, M. Mackenzie and A.J. Craven. Chromium
26 nitrides (CrN, Cr₂N) from solid state metathesis reactions: effects of dilution and nitriding
27 reagent, *J. Mater. Chem.* 8[8] (1998) 1875-1880.
- 28 [51] Z.B. Zhao, Z.U.Rek, S.M. Yalisove, J.C. Bilello, Nanostructured chromium nitride films
29 with a valley of residual stress, *Thin Solid Films* 472 (2005) 96-104.
- 30 [52] D.Wexler, A.Calka and A.Y.Mosbah, Ti-TiN hardmetals prepared by in situ formation of
31 TiN during reactive ball milling of Ti in ammonia, *J. Alloys Com.*,309 (2000) 201-207.
- 32 [53] P. Malet, A.Muñoz-Páez, C.Martín, V.Rives, Sodium-doped V₂O₅/TiO₂ systems: An
33 XRD, DTA, TG/DTG, IR, V-UV, TPR, and XANES study, *J. Catal.*, 134 (1992) 47-57.
- 34 [54] V.López-Flores, M.A.Roldán,C.Real, A.Muñoz Páez,G.R.Castro. Polymorphic
35 transformation from body-centered to face-centered cubic vanadium metal during
36 mechanosynthesis of nanostructured vanadium nitride determined by extended x-ray
37 absorption fine structure spectroscopy, *J.of ppl.phys.* 104, (2008) 023519.
- 38 [55] J.E.Sundgren, H.T.G.Hentzell. A review of the present state of art in hard coatings grown
39 from the vapour phase, *J.vac.sci.technol.A* 4[5] 279 (1986) 2259-2.
- 40 [56] H.C.Barshilia, K.S.Rajam. Nanoindentation and atomic force microscopy measurements
41 on reactively sputtered TiN coatings, *Bull. Mater. Sci.*, 27[1] (2004) 35-41.
- 42
43
44
45
46
47
48
49
50
51
52
53
54
55
56
57
58
59
60
61
62
63
64
65

Figure captions

Figure 1. XRD patterns of sample $Ti_{0.50}V_{0.50}$ at different grinding times.

Figure 2. XRD patterns of sample $Ti_{0.25}V_{0.75}$ at different grinding times.

Figure 3. N-K, Ti-L₂₋₃ and V-L₂₋₃ edges of the differently prepared ternary nitrides.

Figure 4. Normalised XANES spectra of the following absorption edges are shown: a) Ti-K and b)V-K.

Figure 5. SEM micrographs illustrating the morphology of three powder and sintered samples are presented with the following composition: a) $Ti_{0.11}V_{0.89}N_{0.91}$, b) $Ti_{0.50}V_{0.50}N_{0.94}$, and c) $Ti_{0.86}V_{0.14}N_{0.92}$, respectively.

Table captions

Table 1. Parameters of the mechanical treatment of the Ti-V mixture under nitrogen atmosphere: grinding and ignition times and the mechanism.

Table 2. The chemical compositions of the different ternary nitrides prepared.

Table 3. The parameters obtained from the x-ray data of the prepared samples are: size particle, strain and lattice.

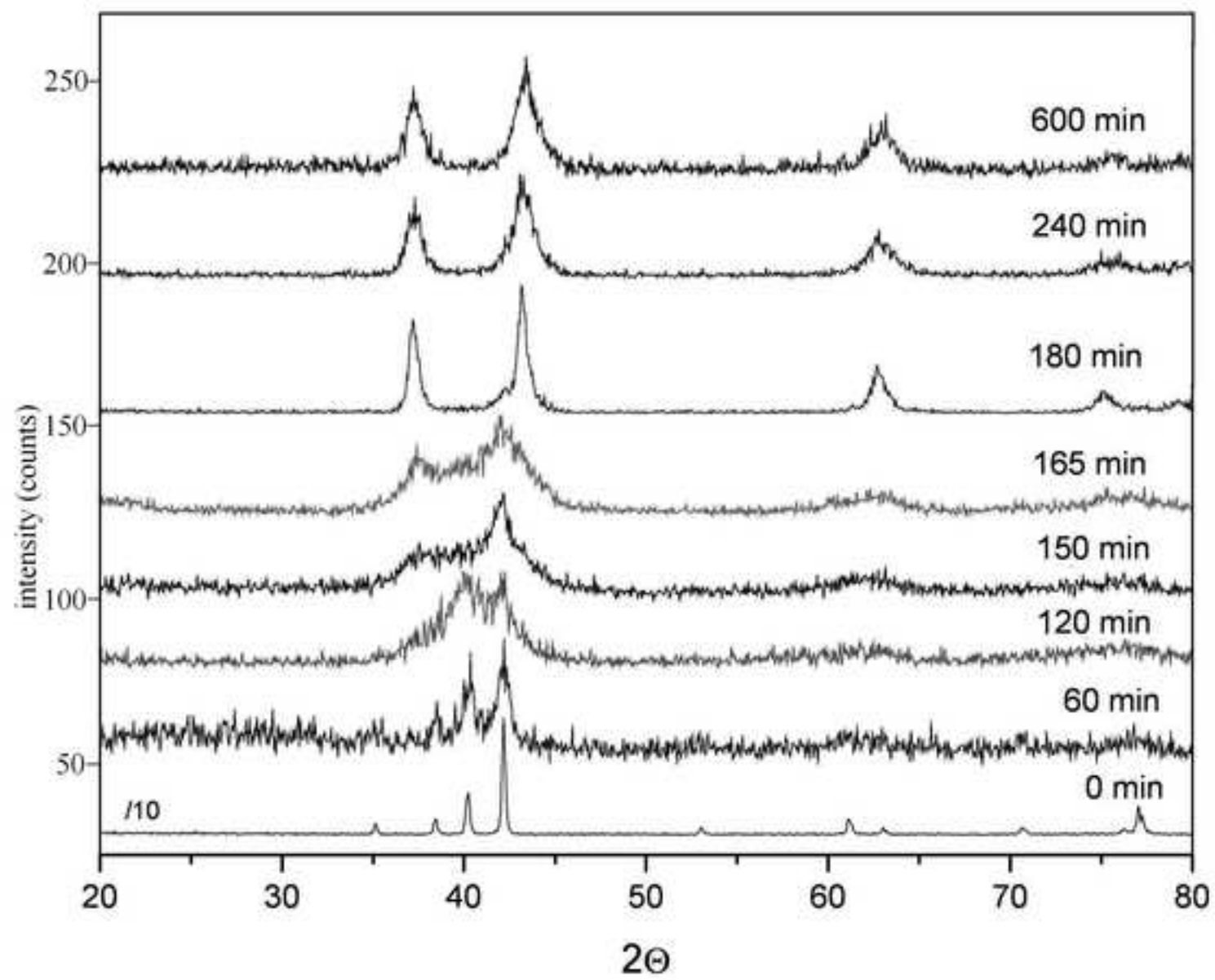
Table 4. A composition comparison of the ternary nitrides obtained from different techniques.

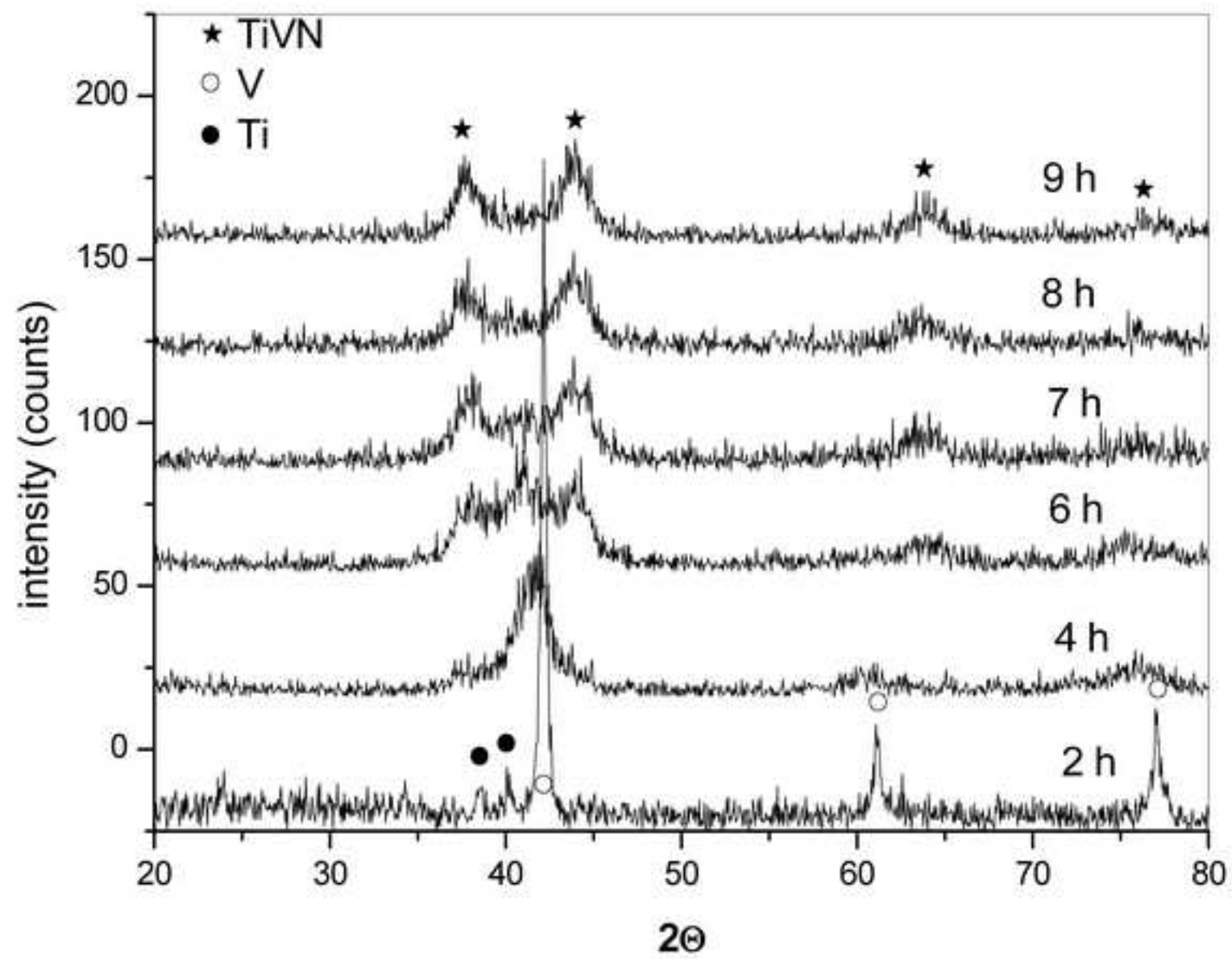
Table 5. The fitting EXAFS parameters of edge K-Ti for sample $Ti_{0.5}V_{0.5}N_{0.94}$. N is the coordination number (fixed to crystalline values), R is the coordination distance (calculated from the lattice parameter), σ^2 is the Debye–Waller factor (independent variable for each shell) and D is the coordination number reduction factor.

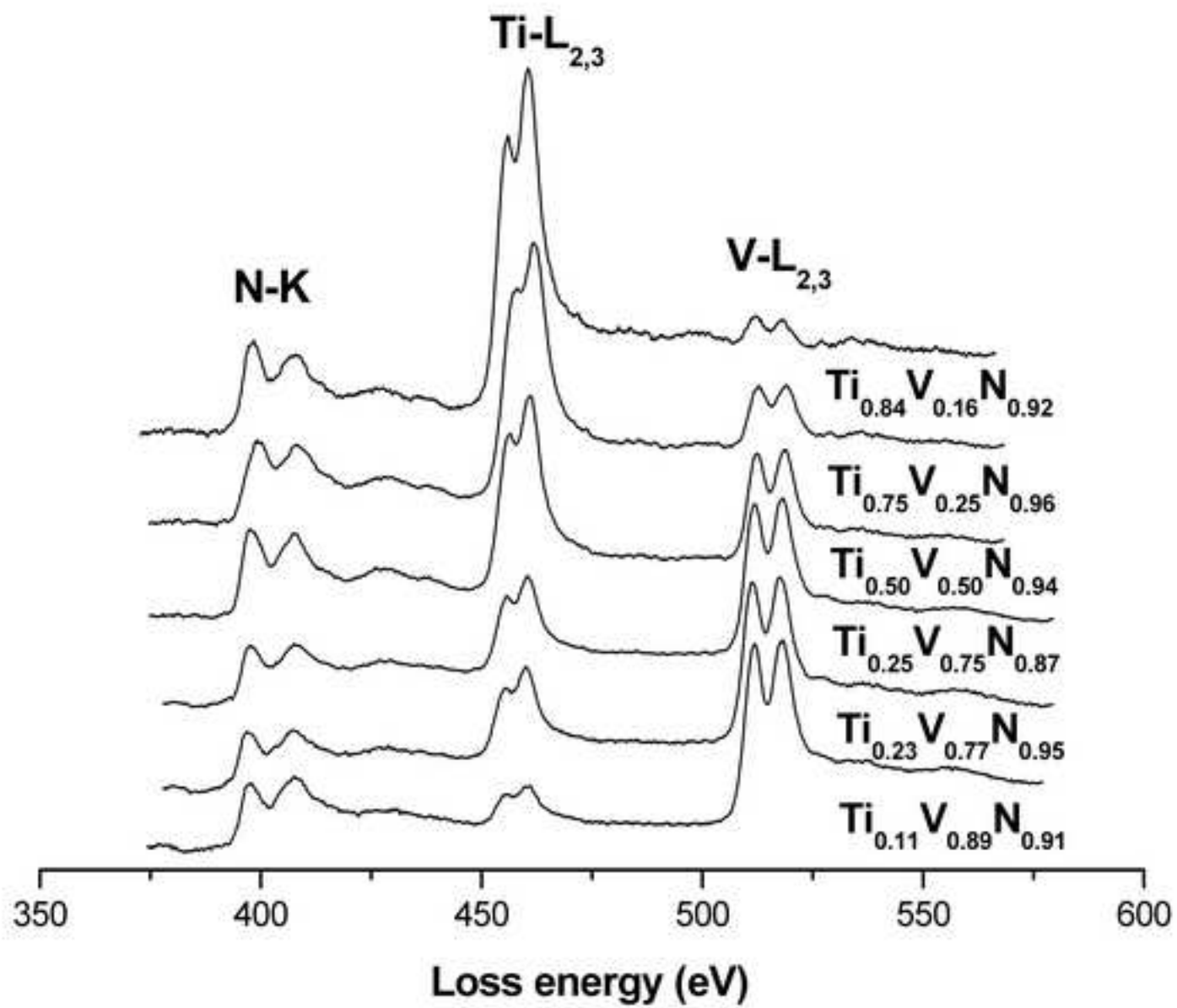
Table 6. The fitting EXAFS parameters of edge K-V for sample $Ti_{0.5}V_{0.5}N_{0.94}$. The variables are described in Table 5.

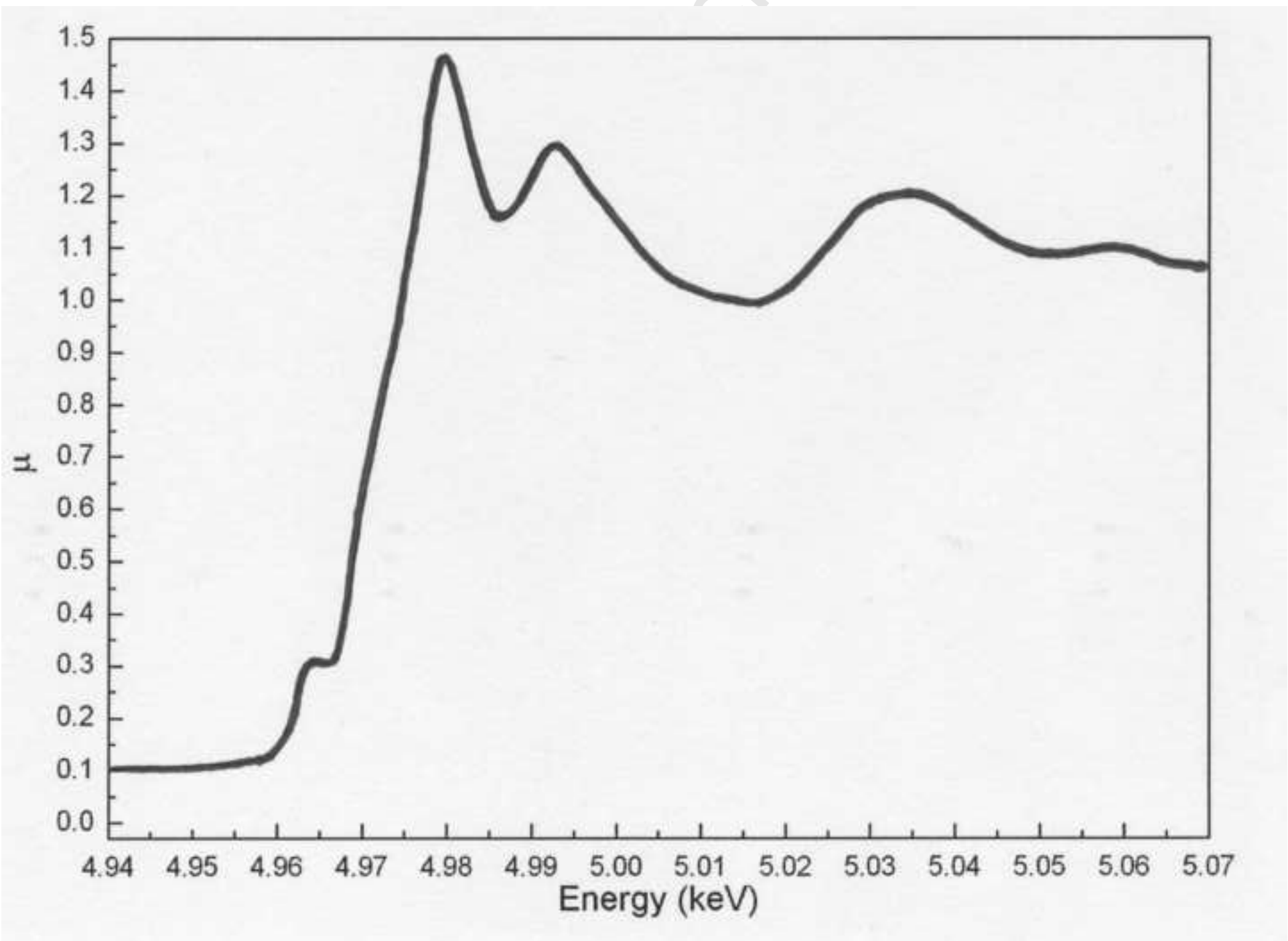
Table 7. The densification and microhardness of the ternary nitrides studied.

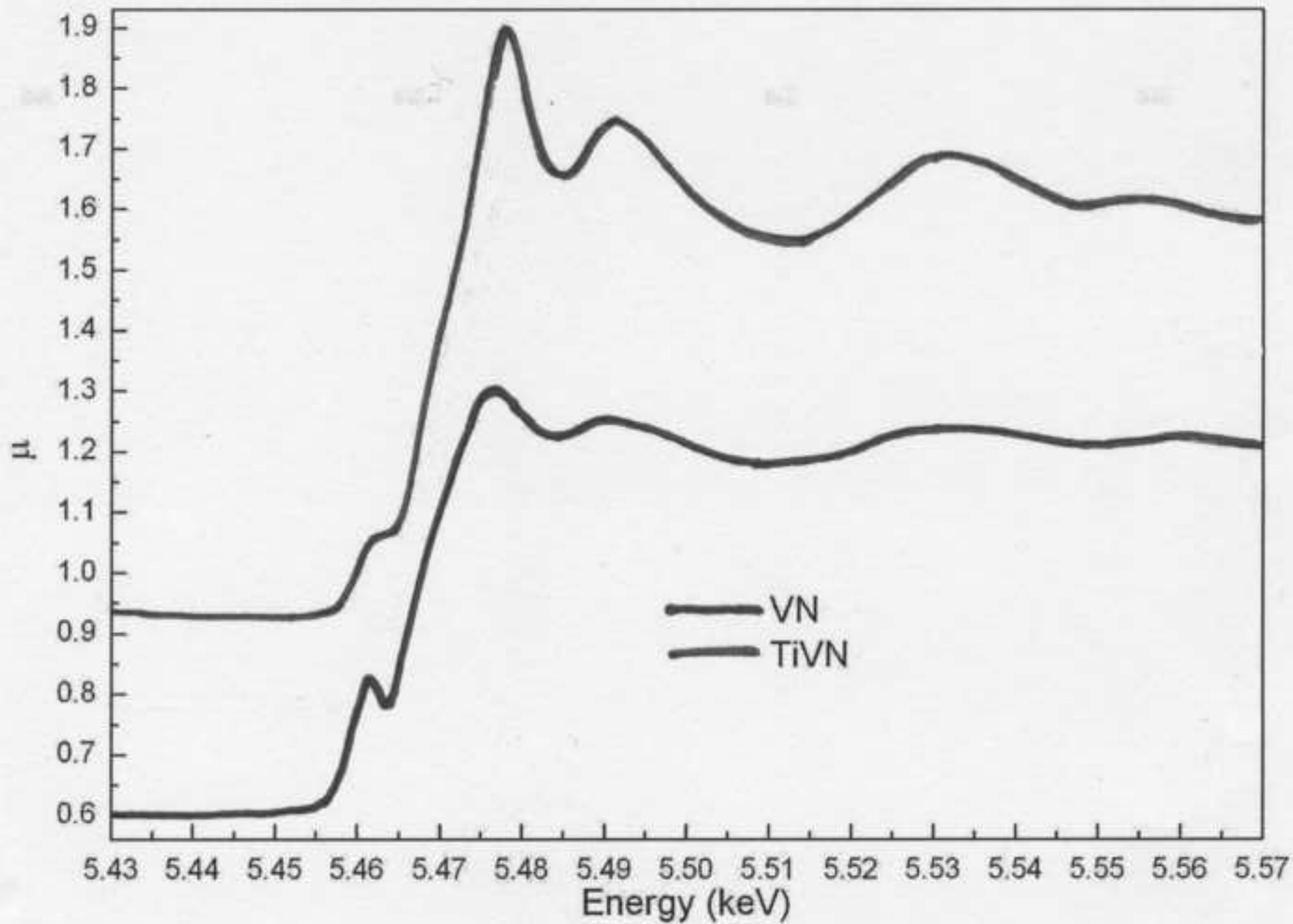
crip

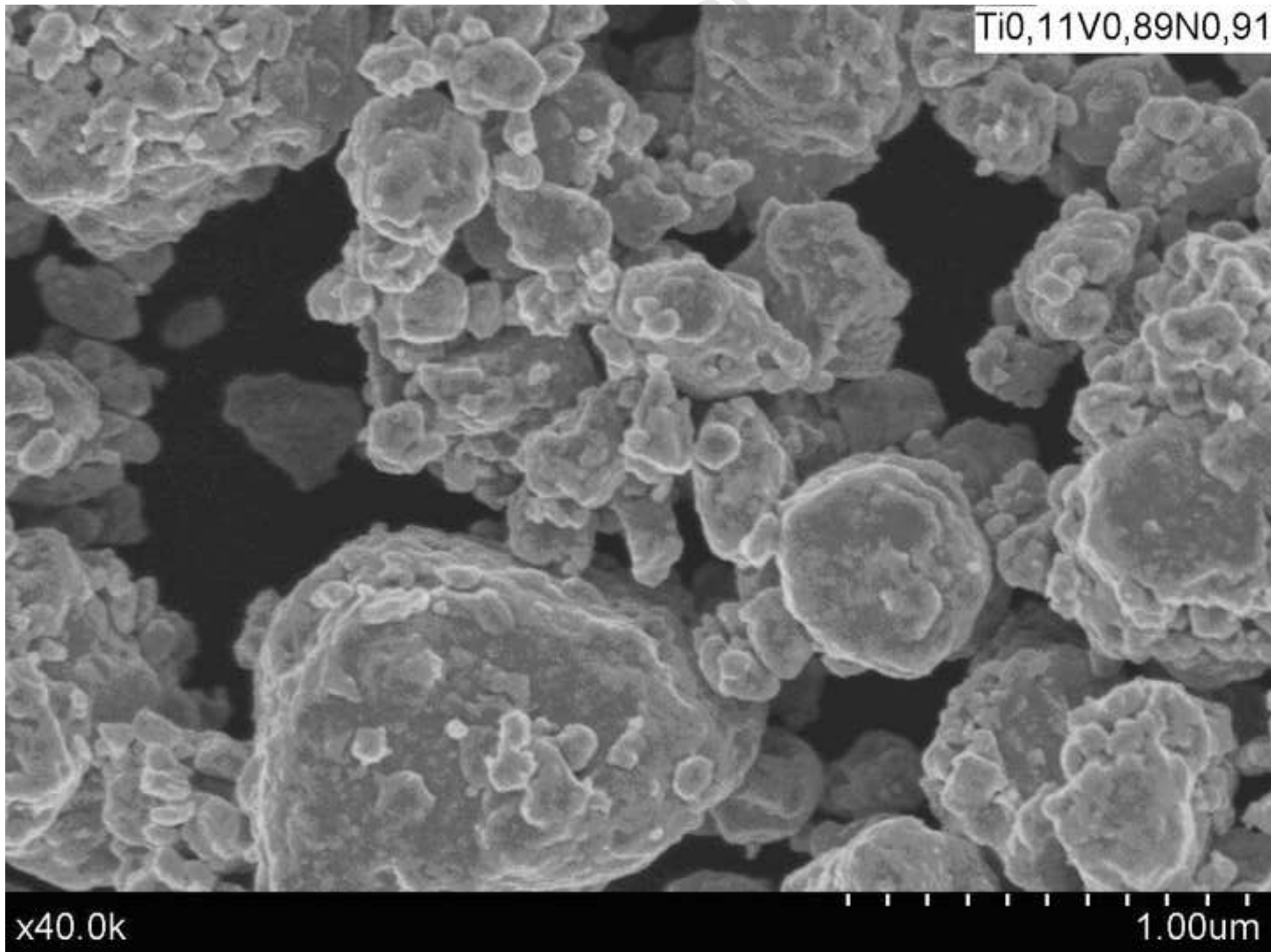


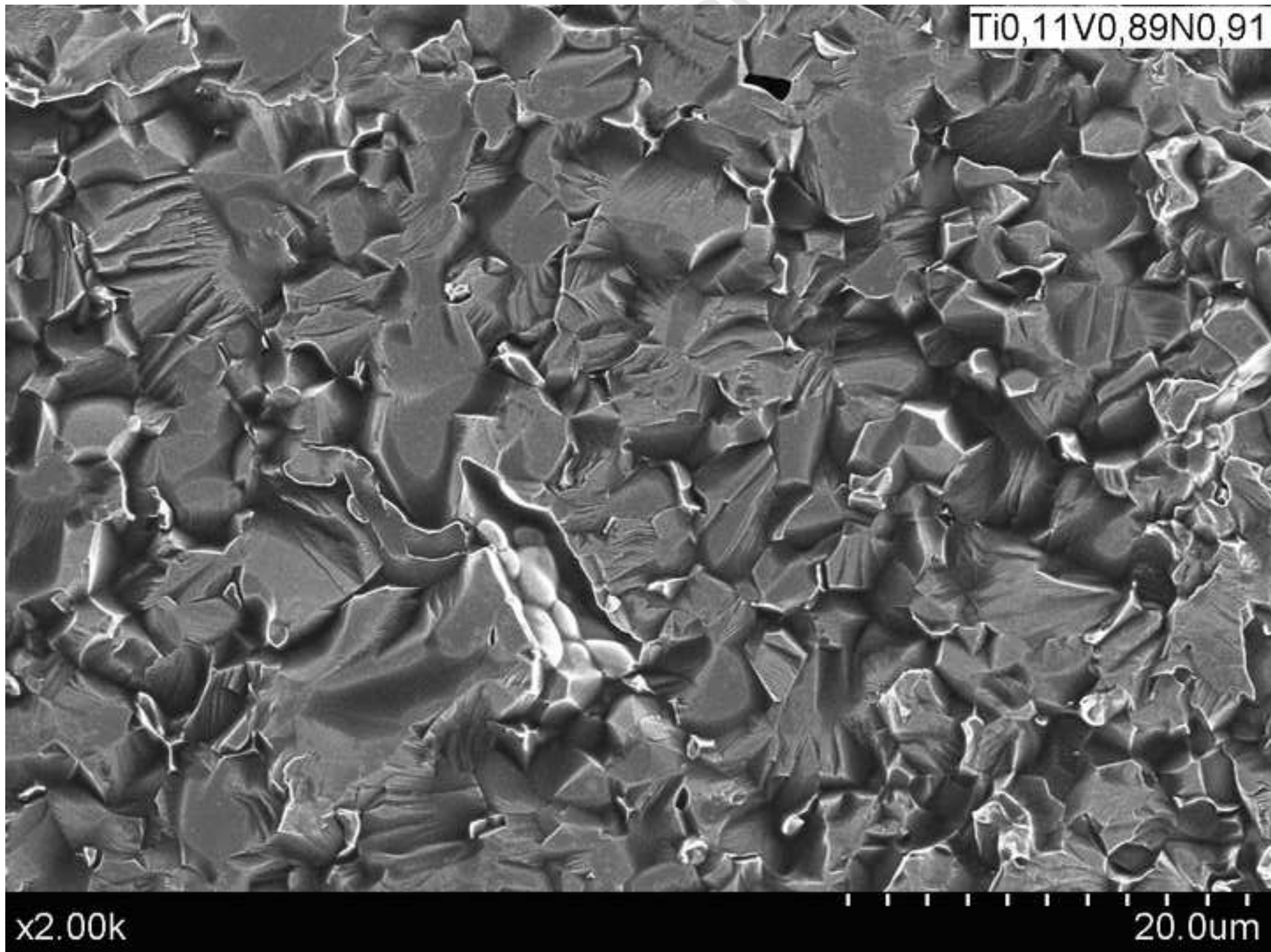


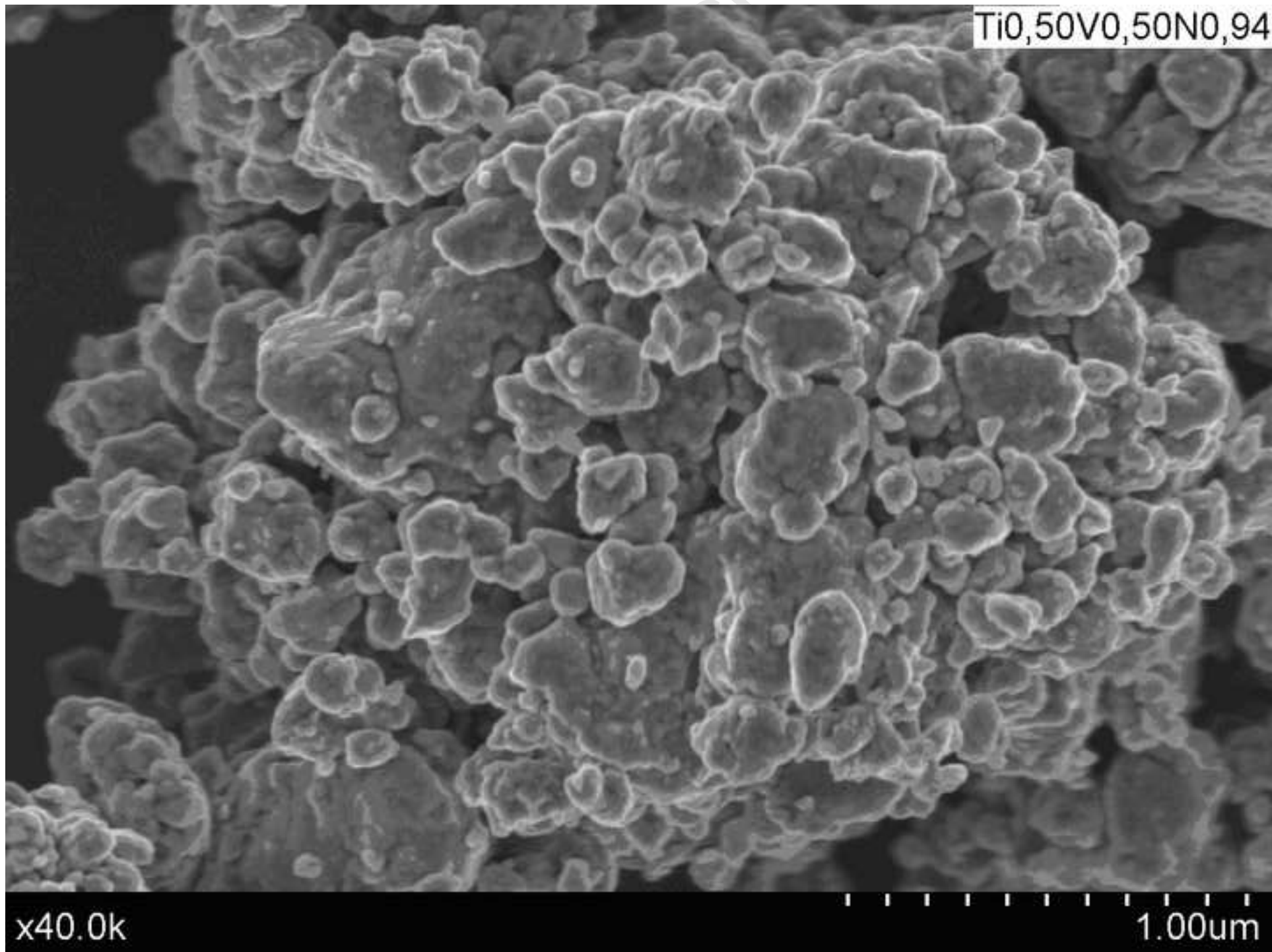


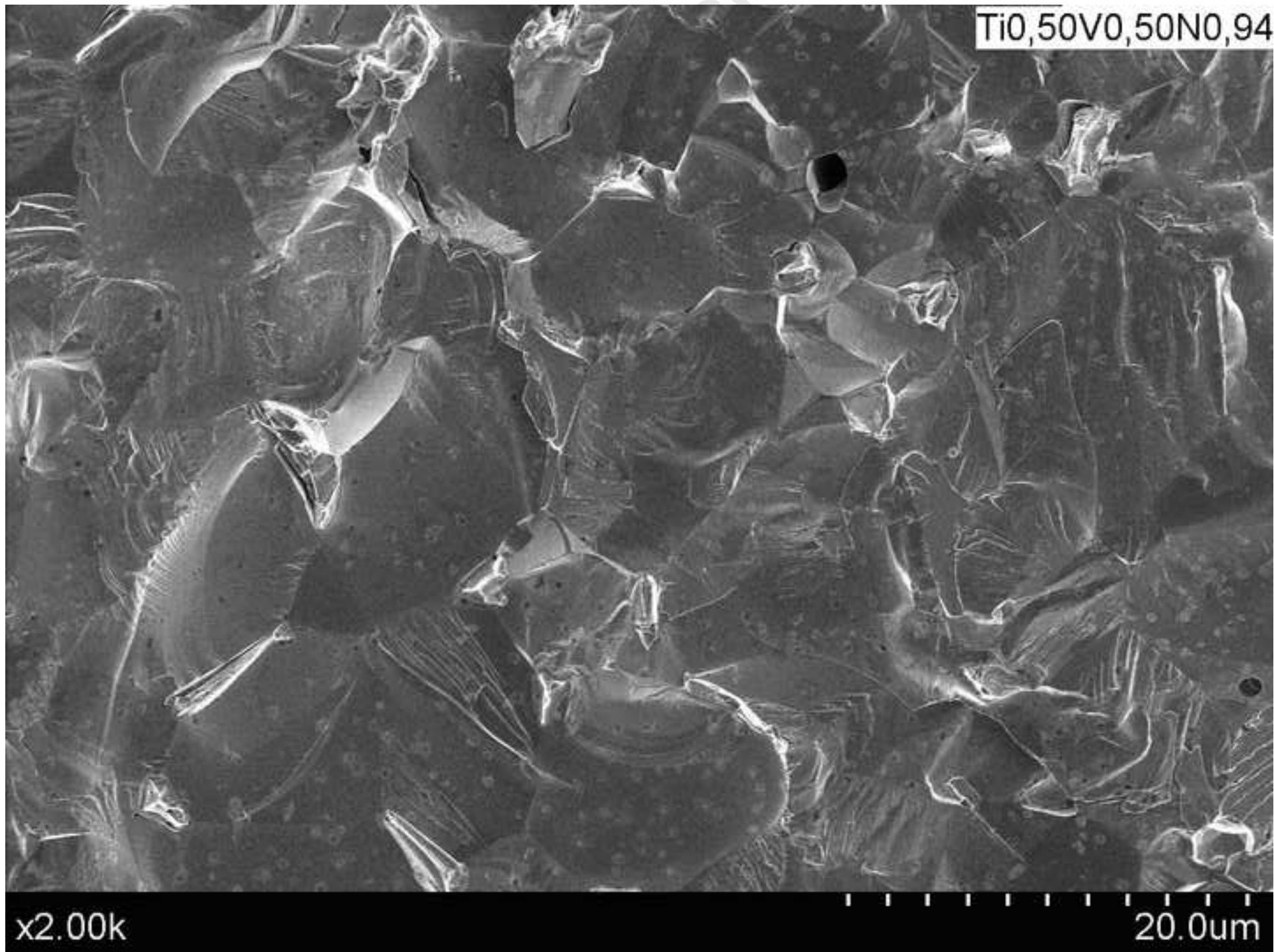


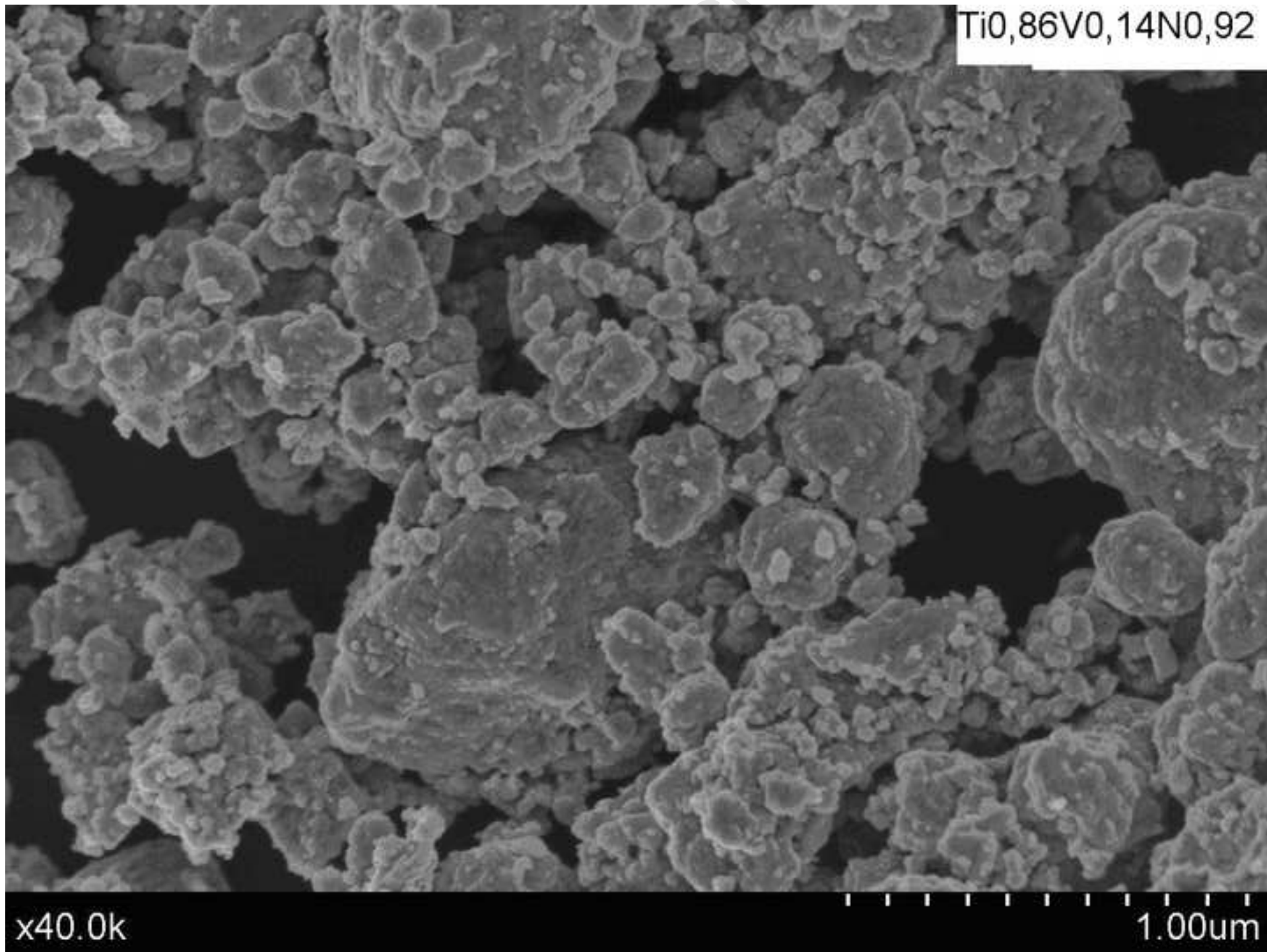


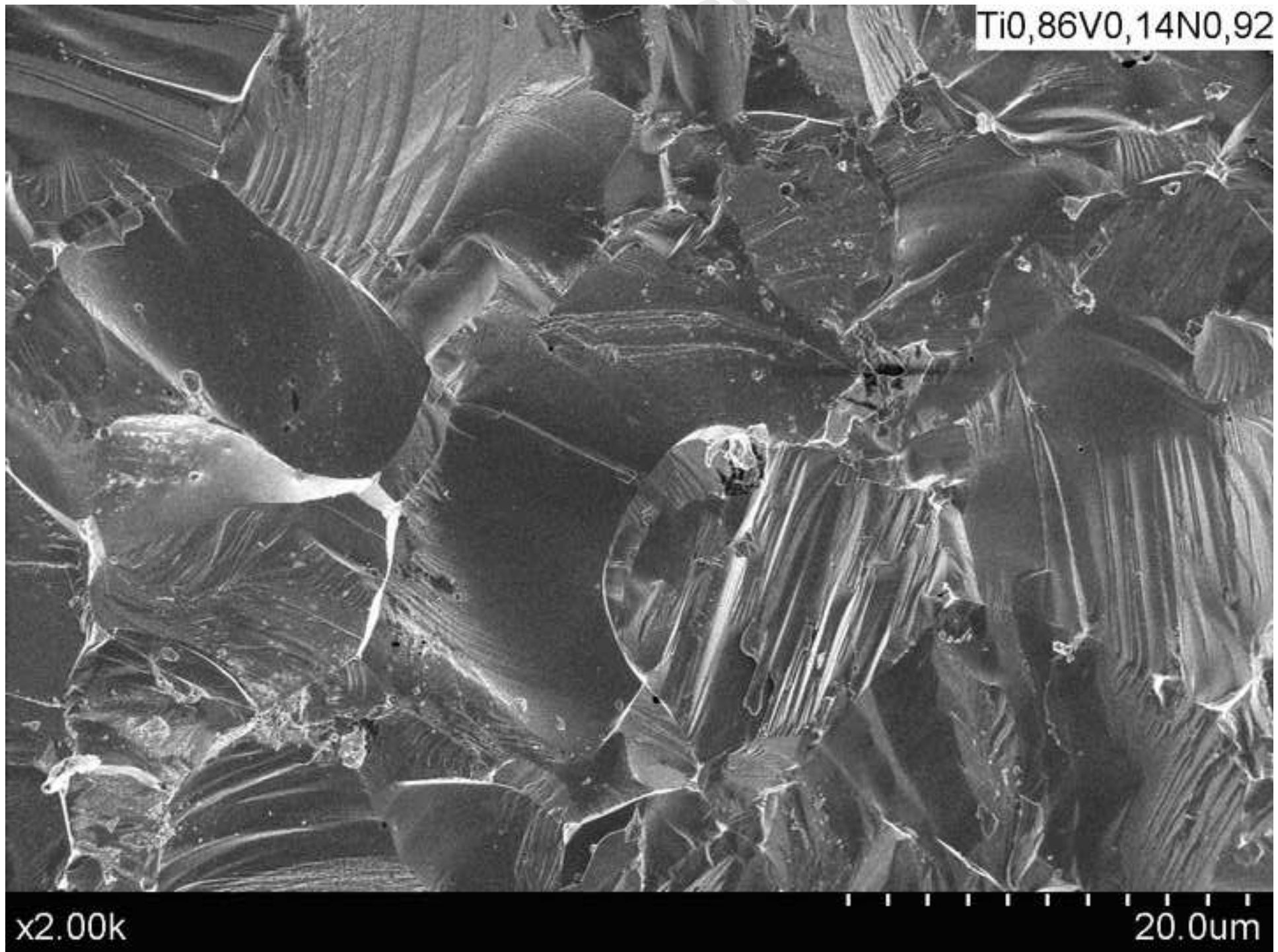












Sample	Mechanism	Ignition time(min)	Grinding time(min)
Ti _{0.86} V _{0.14} N	Combustion	182	200
Ti _{0.75} V _{0.25} N	Combustion	164	200
Ti _{0.50} V _{0.50} N	Combustion	172	540
Ti _{0.25} V _{0.75} N	Diffusion	-	540
Ti _{0.23} V _{0.77} N	Diffusion	-	540
Ti _{0.11} V _{0.89} N	Diffusion	-	540

Accepted Manuscript

Sample	Ti/V (EDX)	Composition	%Fe	%N
Ti _{0.86} V _{0.14} N	6.14	Ti _{0.86} V _{0.14} N _{0.92}	2.5	92
Ti _{0.75} V _{0.25} N	3.00	Ti _{0.75} V _{0.25} N _{0.96}	1.2	96
Ti _{0.50} V _{0.50} N	1.00	Ti _{0.50} V _{0.50} N _{0.94}	2.0	94
Ti _{0.25} V _{0.75} N	0.33	Ti _{0.25} V _{0.75} N _{0.87}	1.8	87
Ti _{0.23} V _{0.77} N	0.30	Ti _{0.23} V _{0.77} N _{0.95}	2.3	95
Ti _{0.11} V _{0.89} N	0.12	Ti _{0.11} V _{0.89} N _{0.91}	1.7	91

Accepted Manuscript

Sample	D(nm)	$\langle e \rangle \times 10^3$	a (Å)	a (Å) Vegard
TiN	-	-	-	4.242
Ti _{0.86} V _{0.14} N _{0.92}	5.7	0.951	4.207	4.227
Ti _{0.75} V _{0.25} N _{0.96}	5.3	0.987	4.217	4.215
Ti _{0.50} V _{0.50} N _{0.94}	5.0	1.432	4.168	4.190
Ti _{0.25} V _{0.75} N _{0.87}	5.5	1.276	4.137	4.165
Ti _{0.23} V _{0.77} N _{0.95}	5.4	0.832	4.128	4.154
Ti _{0.11} V _{0.89} N _{0.91}	5.6	0.765	4.120	4.150
VN	-	-	-	4.140

Accepted Manuscript

Sample	Ti/V EDX	Ti/V EELS	Ti/N TG	Ti/N EELS
Ti _{0.84} V _{0.16} N _{0.92}	6.14	6.00	0.93	0.89
Ti _{0.75} V _{0.25} N _{0.96}	3.00	3.03	0.78	0.73
Ti _{0.50} V _{0.50} N _{0.94}	1.00	1.02	0.53	0.57
Ti _{0.25} V _{0.75} N _{0.87}	0.27	0.33	0.29	0.28
Ti _{0.23} V _{0.77} N _{0.95}	0.30	0.30	0.24	0.19
Ti _{0.11} V _{0.89} N _{0.91}	0.12	0.13	0.12	0.09

Accepted Manuscript

Sample	TiN-fcc (90%)				Ti Metal-fcc (10%)	
D	0.56				0.99	
Lattice parameter	4.17				4.27	
shell	1^a (N)	2^a (Ti)	3^a (N)	4^a (Ti)	1^a	2^a
N	6	12	8	6	12	6
R (Å)	2.09	2.95	3.61	4.17	3.02	4.27
σ (Å²)	0.0037	0.014	0.020	0.023	0.003	0.007

Sample	VN-fcc (75%)				V Metal-bcc (25%)	
D	0.73				0.99	
Lattice parameter	4.17				3.17	
Shell	1^a (N)	2^a (V)	3^a (N)	4^a (V)	1^a	2^a
N	6	12	8	6	8	6
R (Å)	2.09	2.95	3.61	4.17	3.02	3.17

Accepted Manuscript

Sample	Densificación (%)	Microhardness (Hv)	Microhardness (Hv). ref. 47
Ti_{0.86}V_{0.14}N_{0.92}	96	1336	1355
Ti_{0.75}V_{0.25}N_{0.96}	94	1425	1300
Ti_{0.50}V_{0.50}N_{0.94}	96	1376	1100
Ti_{0.25}V_{0.75}N_{0.87}	98	1166	1141
Ti_{0.23}V_{0.77}N_{0.95}	97	1157	1140
Ti_{0.11}V_{0.89}N_{0.91}	96	1277	1262